

# Pseudo Anomalies Are All You Need: Diffusion-Based Generation for Weakly-Supervised Video Anomaly Detection

Satoshi Hashimoto, Hitoshi Nishimura, Yanan Wang, and Mori Kurokawa  
KDDI Research, Inc.



Figure 1. Our PA-VAD framework generates class-aware pseudo-abnormal videos (e.g., Explosion, Road Accidents, Assault) from only a small set of normal images. These controllable pseudo anomalies provide scalable and diverse supervision, eliminating the need for real abnormal data—the primary bottleneck in weakly supervised VAD—and substantially expanding the range of trainable abnormal patterns.

## Abstract

Deploying video anomaly detection in practice is hampered by the scarcity and collection cost of real abnormal footage. We address this by training without any real abnormal videos while evaluating under the standard weakly supervised split, and we introduce PA-VAD, a generation-driven approach that learns a detector from synthesized pseudo-abnormal videos paired with real normal videos, using only a small set of real normal images to drive synthesis. For synthesis, we select class-relevant initial images with CLIP and refine textual prompts with a vision-language model to improve fidelity and scene consistency before invoking a video diffusion model. For training, we mitigate excessive spatiotemporal magnitude in synthesized anomalies by a domain-aligned regularized module that combines domain alignment and memory usage-aware updates. Extensive experiments show that our approach reaches 98.2% on ShanghaiTech and 82.5% on UCF-Crime, surpassing the strongest real-abnormal method on ShanghaiTech by +0.6% and outperforming the UVAD state-of-the-art on

UCF-Crime by +1.9%. The results demonstrate that high-accuracy anomaly detection can be obtained without collecting real anomalies, providing a practical path toward scalable deployment.

## 1. Introduction

Ensuring public safety and order has driven extensive research on video anomaly detection (VAD) in computer vision. VAD aims to identify abnormal events such as assaults, traffic accidents, and theft in surveillance videos. Prior works span two main families: (i) unsupervised VAD (UVAD), which trains only on normal data [6, 9, 10, 15, 17, 18, 25, 26, 30]; (ii) weakly supervised VAD (WVAD), which relies on normal and abnormal videos with video-level labels [5, 7, 11, 16, 19, 21, 22, 24, 27, 28, 31, 32].

Despite rapid progress, deployment remains challenging. UVAD methods can be brittle under distribution shift and label noise, whereas WVAD approaches typically assume access to substantial real abnormal footage, which is costly and often constrained by safety, privacy, or rarity. A com-

plementary direction synthesizes pseudo anomalies to ease data scarcity [3, 14]. Yet, in most cases the synthesized clips supplement rather than replace real anomalies, and the synthesis is driven by rule-based edits or narrow generative priors, so the reliance on real abnormal data is reduced but not removed.

**Our approach.** We introduce **PA-VAD**, a generation-driven framework that learns an anomaly detector from pseudo-anomalous videos synthesized from a small set of real normal images. Training uses no real abnormal videos, while evaluation follows the conventional weakly supervised splits. Unlike prior pseudo-anomaly works that mainly supplement real anomalies and rely on heuristic edits or narrow generators, our synthesis pipeline is designed to replace real anomalies: we select class-relevant seed images with CLIP and perform VLM-based prompt rewriting before driving a video diffusion model, which improves fidelity and scene consistency without manual prompt search.

To address deployment barriers on the learning side—robustness under shift and MIL bias caused by inflated feature magnitudes in synthesized clips—we introduce a Domain-Aligned Regularized Module (DARM) that combines (i) domain adaptation between real Normal and pseudo-Normal streams and (ii) usage-aware slot updates. This design reduces covariate shift, curbs magnitude-driven bias, stabilizes training, and yields stronger discrimination.

We conduct extensive experiments on multiple benchmarks, showing that our approach not only outperforms state-of-the-arts UVAD baselines but also surpasses competitive methods that rely on real abnormal videos, while dramatically reducing data collection costs.

- We propose a generation-driven VAD framework that trains without real abnormal videos while evaluating under standard weakly supervised splits, substantially reducing data collection costs.
- We propose the Class-Aware Pseudo-Anomaly Generator (CA-PAG), a video diffusion-based pseudo-anomaly generator that attains high-fidelity abnormal videos through CLIP-guided initial image selection and VLM-driven prompt refinement.
- We propose the Domain-Aligned Regularized Module (DARM), an adaptive memory module that exploits the diversity of synthesized anomalies and corrects the large-magnitude bias characteristic of generated videos via domain adaptation and usage-aware updates.
- Through comprehensive experiments on multiple datasets, we demonstrate state-of-the-art results against UVAD methods and show that our approach can surpass strong methods that depend on real abnormal videos.

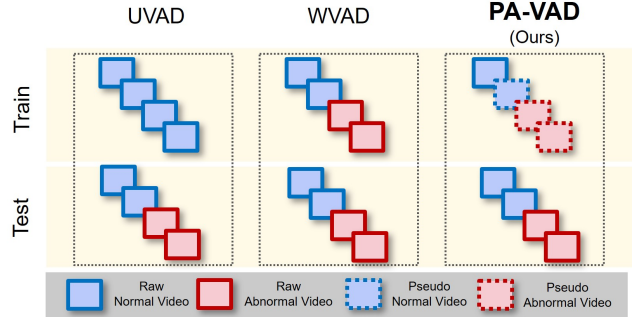


Figure 2. Overview of our framework. PA-VAD trains on real Normal and diffusion-generated pseudo videos (no real Abnormal) and is evaluated on standard splits with real Normal/Abnormal.

## 2. Related Work

### 2.1. Video Anomaly Detection

We group prior work into two families—unsupervised (UVAD) and weakly supervised (WVAD) based methods—and summarize their techniques and limitations. In UVAD, classical approaches include dictionary learning on normal-only data [15] and prediction/reconstruction paradigms [9, 10, 17, 18, 25, 26, 30]. Recent methods that integrate prediction with reconstruction have proven effective; to explicitly address small-scale anomalies and background interference, MGSTRL learns multi-grained spatio-temporal representations via three proxy tasks—continuity judgment, discontinuity localization, and contrastive missing-frame estimation in feature space—achieving state-of-the-art results, especially on small-scale anomalies. [30] A persistent deployment issue for UVAD is the assumption that training covers all normal variations, which rarely holds in the wild. When previously unseen normal patterns arise due to camera/view changes or noise, UVAD methods tend to suffer from false positives.

In contrast, WVAD has become popular as a practical discriminative framework trainable with weak video-level labels. A large body of work explores architectures using video-level supervision to infer frame-level anomalies [5, 11, 16, 19, 21, 22, 27, 31, 32]. Sultani *et al.* [16] introduced a MIL-based training scheme under weak labels. Each video is split into non-overlapping segments and represented as a bag of instances: a normal bag  $\tilde{B}_n = \{\mathbf{f}_n^i\}_{i=1}^m$  and an abnormal bag  $\tilde{B}_a = \{\mathbf{f}_a^i\}_{i=1}^l$ , where  $\mathbf{f} \in \mathbb{R}^K$  denotes a  $K$ -dimensional feature vector and  $m, l$  are the numbers of segments. A detector  $\mathcal{D}$  outputs an anomaly score  $s = \mathcal{D}(\mathbf{f})$  for each segment. Under the MIL assumption, the detector is optimized so that the maximum score in abnormal bags exceeds that in normal bags, using the ranking loss:

$$\mathcal{L}_{\text{MIL}} = \max \left( 0, 1 - \max_{i \in \tilde{B}_a} s_a^i + \max_{i \in \tilde{B}_n} s_n^i \right). \quad (1)$$

Unlike UVAD, such weak supervision learns discrimi-

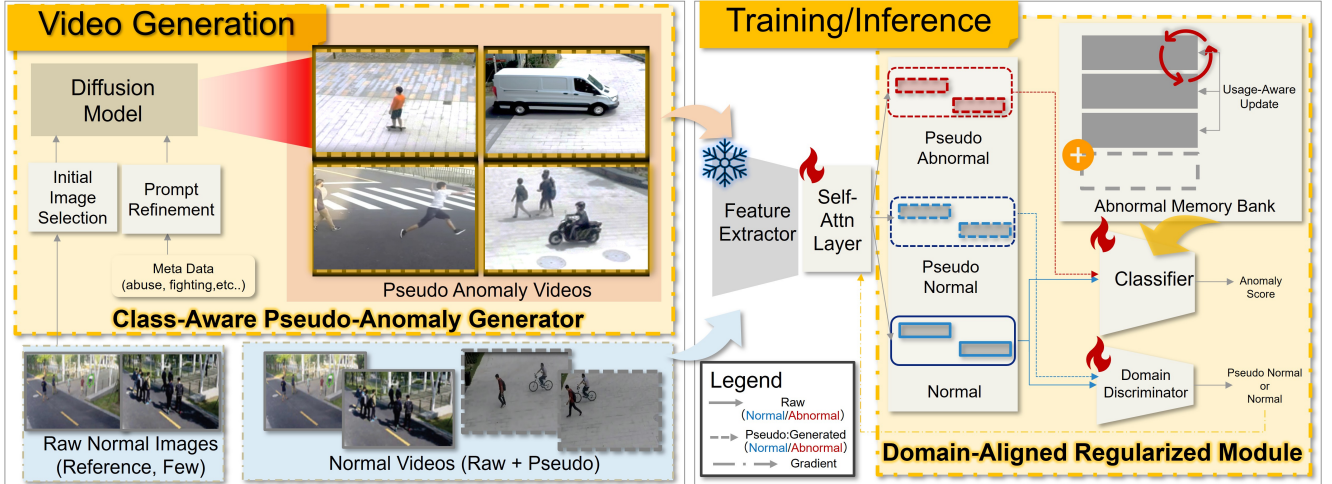


Figure 3. Overview of our framework. Starting from a small set of real normal images and class texts, we synthesize pseudo-abnormal videos via an image-to-video diffusion process, then train a classifier on real normal and synthesized pseudo-abnormal videos. An Domain-Aligned Regularized Module—designed to account for the characteristic large spatiotemporal magnitude of synthesized anomalies—mitigates Multiple Instance Learning (MIL) bias and enables accurate detection.

native representations and tends to be more robust to multi-scene settings and complex backgrounds. Recently, WVAD methods have adopted vision–language models (VLMs) for better interpretability. Du *et al.* [7] target causal understanding of abnormal events using hard/soft prompts. Zhang *et al.* [28] fine-tune VLM on large captioned datasets and report leading performance. However, both WVAD approaches typically presuppose large-scale collection of real abnormal videos, which can be costly and constrained by safety and privacy, limiting practical deployment.

## 2.2. Pseudo Video Generation

Several works have explored generating pseudo data to boost VAD. Cai *et al.* [3] integrate video generation into weakly supervised training by synthesizing text-conditioned pseudo anomalies mixed with real abnormal videos. This alleviates but does not eliminate reliance on real anomalies, as full real sets remain used during training. Rai *et al.* [14] generate pseudo anomalies for UVAD by inpainting or perturbing normal videos, but rely on hand-crafted rules that limit diversity and realism.

Recent advances in diffusion models have produced powerful video generators. Two major conditions are common: text-to-video (T2V), which directly synthesizes videos from text prompts, and image-to-video (I2V), which extends a static image over time while preserving spatial structure under a prompt. Wan 2.2 is a diffusion-Transformer framework with noise-stage Mixture-of-Experts and highly compressed latent representations [20]. VideoCrafter2 extends Stable Diffusion to videos and trains with a mixture of low-quality videos and synthetic high-quality images [4]. Stable Video Diffusion establishes a three-stage curriculum spanning text–image

pretraining, video pretraining, and high-quality video fine-tuning [2]. While these models are strong general-purpose generators, they are not tailored for anomaly synthesis; prompting to obtain rare abnormal behaviors is challenging and typically requires careful search and conditioning.

## 3. Proposed Method

Motivated by the above limitations, we propose **PA-VAD**, a generation-driven approach that synthesizes pseudo-abnormal videos from a small number of real normal images and trains a detector on them. An overview is given in Fig. 3. Our framework comprises two synergistic components: (i) a *Class-Aware Pseudo-Anomaly Generator* and (ii) an *Domain-Aligned Regularized Module*. We detail each module below.

### 3.1. Class-Aware Pseudo-Anomaly Generator

The goal is to synthesize pseudo-abnormal videos from only a small set of real normal images and class metadata (abnormal class names) by driving a video diffusion model. We adopt an image-to-video (I2V) inference process conditioned on (a) a initial image and (b) a textual prompt. A central challenge is the covariate shift between synthesized anomalies and real data: prior synthesis for VAD either mixes generated clips with real abnormal videos [3] or perturbs real images/videos [14], which keeps the domain gap relatively small. In contrast, because our aim is to eliminate reliance on real abnormal footage altogether, *reducing this gap while preserving quality* is crucial. We therefore introduce the Class-Aware Pseudo-Anomaly Generator (CAPAG), whose synthesis is controlled by two levers: (1) **initial image selection** to anchor the generation near the target class domain, and (2) **prompt refinement** to tailor textual



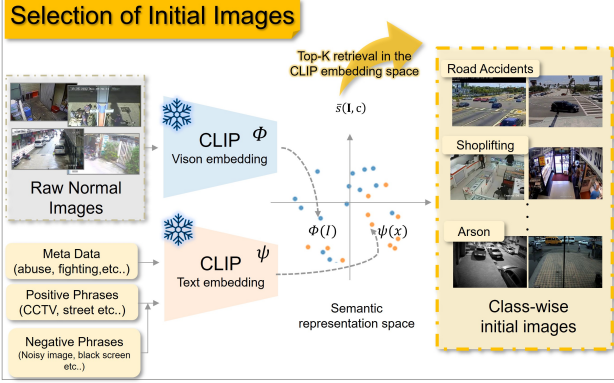


Figure 4. Initial image selection in the vision-text space. We score normal images using a class text with positive phrases and subtract an aggregated negative similarity, then take the Top- $K$  per class.

conditioning to the chosen initial image via zero-shot vision-language reasoning.

### 3.1.1. Initial Image Selection

Naively sampling initial images at random from the normal set risks large domain gaps for certain classes (e.g., selecting an indoor home scene for the target class “Road Accident” in UCF-Crime [16]). Instead, we propose to select *class-relevant* inits with CLIP [13] using a Top- $K$  strategy in the joint vision-text space (Fig. 4).

Concretely, given a class label  $x_c$ , we augment it with positive phrases  $g_{pos}$  to enforce surveillance-style attributes such as camera footage and CCTV, and introduce a set of negative phrases  $g_{neg}$  to suppress nuisances such as black screens or channel logos. Let  $\Phi$  and  $\psi$  denote the CLIP image and text encoders. Please refer to the supplementary material for the detailed description of each phase. Define unit-normalized embeddings  $\hat{\mathbf{v}}(\mathbf{I}) = \Phi(\mathbf{I})/|\Phi(\mathbf{I})|_2$  and  $\hat{\mathbf{t}}(u) = \psi(u)/|\psi(u)|_2$ . We form a single positive text by concatenating the class name with positives,  $t_c = \text{concat}(x_c, g_{pos})$  and compute the positive similarity:

$$s_{pos}(\mathbf{I}, c) = \langle \hat{\mathbf{v}}(\mathbf{I}), \hat{\mathbf{t}}(t_c) \rangle. \quad (2)$$

We compute each negative similarity:

$$s_{neg}(\mathbf{I}) = \langle \hat{\mathbf{v}}(\mathbf{I}), \hat{\mathbf{t}}(n) \rangle. \quad (3)$$

The final score balances class affinity and nuisance suppression,

$$\tilde{s}(\mathbf{I}, c) = s_{pos}(\mathbf{I}, c) - \lambda s_{neg}(\mathbf{I}), \quad \lambda \in [0, 1], \quad (4)$$

and we select the Top- $K$  images with highest  $\tilde{s}(\mathbf{I}, c)$  as the initial set  $\text{TopK}_c$  for class  $c$ .

We optionally apply scene balancing before and after scoring to reduce bias while preserving high-score candidates. First, we sub-sample images per scene  $s$  proportionally to  $\text{count}(s)^\alpha$  to obtain a smoothed pool. Then, for each

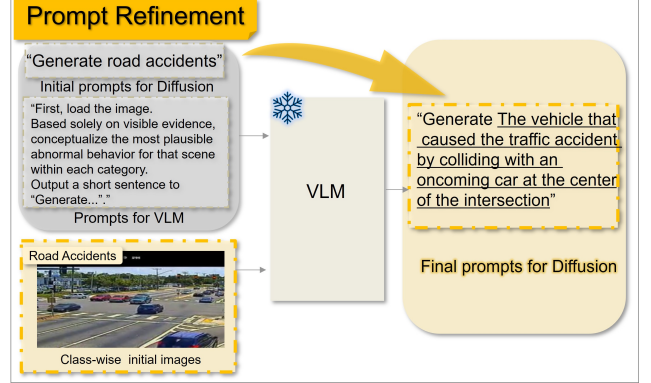


Figure 5. Prompt refinement. A VLM extracts scene- and object-aware cues from the initial image under a class-aware instruction and produces concise abnormal descriptions, which are concatenated with template phrases before driving the diffusion model.

class, we reserve a minimum quota per scene and fill the remaining slots by global ranking with  $\tilde{s}(\mathbf{I}, c)$ .

### 3.1.2. Prompt Refinement for Pseudo Anomalies

Using a raw class name as a prompt is simple but often ambiguous, which harms generation consistency and text-video alignment [8, 12]. Exhaustive manual search, however, is impractical. We therefore refine prompts with a vision-language model (VLM) by extracting objects and scene cues from each initial image and turning them into concise, class-consistent abnormal descriptions (Fig. 5).

Given initial images  $\{\mathbf{I}_c^{(k)}\}_{k=1}^K$  for class  $c$ , a class text  $x_c$ , and a refinement instruction  $g_{vlm}$ , the VLM produces short candidate phrases:

$$\hat{s}_c^{(k)} = \mathcal{G}_\varphi(\mathbf{I}_c^{(k)}, g_{vlm}, x_c). \quad (5)$$

To standardize camera and rendering attributes and suppress artifacts, each phrase is concatenated with a set of template prompts  $g_{tem}$  (e.g., *natural movement*, *fixed camera*):

$$p_c^{(k)} = \text{concat}(\hat{s}_c^{(k)}, g_{tem}). \quad (6)$$

Finally, the video diffusion model  $\mathcal{G}_\theta$  is conditioned on the refined prompt and the corresponding initial image to synthesize a pseudo-abnormal clip:

$$\tilde{\mathbf{V}}_c^{(k)} = \mathcal{G}_\theta(p_c^{(k)}, \mathbf{I}_c^{(k)}). \quad (7)$$

Please refer to the supplementary material for the detailed description of refinement instruction.

## 3.2. Domain-Aligned Regularized Module

This module trains and infers an anomaly detector using synthesized pseudo-abnormal videos  $\tilde{\mathbf{V}}$  and real normal videos  $\mathbf{V}$ . When we simply plug synthesized videos into existing weakly supervised pipelines, we observe a characteristic failure mode: generated clips tend to exhibit excessive motion and viewpoint changes, inflating feature norms



Table 1. Mean feature norm comparison between real and pseudo anomalies (UCF-Crime, I3D features).

	Real	Pseudo
Mean norm	20.52	23.03

and biasing MIL Top- $k$  optimization toward a few high-magnitude pseudo instances. This bias induces a covariate shift at test time against real anomalies and degrades sensitivity. Table 1 reports the mean I3D feature norms on UCF-Crime for real vs. pseudo anomalies.

To counter this and faithfully exploit the diversity of synthesized data, we introduce the Domain-Aligned Regularized Module (DARM) with two components: (i) **Domain alignment**: a DANN-based objective that aligns real/pseudo normal distributions to reduce covariate shift; (ii) **Usage-aware memory update**: an update rule that pulls under-utilized slots toward their responsibility-weighted centers to rebalance coverage across abnormal modes.

The domain alignment term is applied to mean-pooled features of real normal and pseudo-normal streams. By encouraging domain-invariant representations via gradient reversal, it reduces systematic magnitude shifts between real and pseudo data, preventing pseudo anomalies from dominating MIL Top- $k$  solely due to inflated norms.

The usage-aware memory update balances the abnormal prototypes. It computes per-slot usage from soft assignments and updates under-utilized slots toward their responsibility-weighted centers, mitigating the tendency of a few high-norm slots to monopolize MIL Top- $k$  selection. We follow the UR-DMU[32] classifier, which provides a GL-MHSA-based encoder, dual (normal/abnormal) memory banks for prototype separation, and a MIL scoring head with uncertainty control. Adding the DARM objectives on top of this backbone effectively suppresses the MIL bias caused by excessive spatiotemporal magnitude in synthesized anomalies while preserving representation diversity across abnormal prototypes.

**Formulation.** Given a video, a feature extractor  $\Phi_{\text{vid}}$  produces segment features  $\mathbf{f} = \Phi_{\text{vid}}(\mathbf{V}) \in \mathbb{R}^{T \times D}$ . We embed them with temporal convolution and self-attention to obtain  $\tilde{\mathbf{f}} \in \mathbb{R}^{B \times T \times d}$ .

$$\tilde{\mathbf{f}} = \text{SelfAttn}(\text{Temporal}(\mathbf{f})). \quad (8)$$

Let  $\mathbf{M}_A, \mathbf{M}_N \in \mathbb{R}^{K \times d}$  denote abnormal and normal memory banks. Their memory-guided augmentations are  $\mathbf{h}_A(\tilde{\mathbf{f}})$  and  $\mathbf{h}_N(\tilde{\mathbf{f}})$ . We concatenate these with  $\tilde{\mathbf{f}}$  and predict frame-wise anomaly scores  $\hat{\mathbf{a}}$ :

$$\hat{\mathbf{a}} = \sigma(\mathbf{W} [\tilde{\mathbf{f}}; \mathbf{h}_A(\tilde{\mathbf{f}}) + \mathbf{h}_N(\tilde{\mathbf{f}})] + \mathbf{b}). \quad (9)$$

Let  $\mathcal{S}_{\text{abn}}$  be indices of abnormal embeddings and  $\tilde{\mathbf{f}}_{\text{abn}} = \tilde{\mathbf{f}}[\mathcal{S}_{\text{abn}}]$ . Unfolding over time yields  $\mathbf{Z} \in \mathbb{R}^{(B_a T) \times d}$ . Define row-wise  $\ell_2$  normalization by  $\mathbf{D}_Z = \text{diag}(\|\mathbf{Z}_1\|_2, \dots, \|\mathbf{Z}_{B_a T}\|_2)$  and  $\tilde{\mathbf{Z}} = \mathbf{D}_Z^{-1} \mathbf{Z}$ . Similarly, with  $\mathbf{D}_M = \text{diag}(\|\mathbf{m}_1\|_2, \dots, \|\mathbf{m}_K\|_2)$ , let  $\tilde{\mathbf{M}}_A =$

$\mathbf{D}_M^{-1} \mathbf{M}_A$ . With temperature  $\tau > 0$ , we define the assignment matrix and slot usage as:

$$\mathbf{Q} = \text{softmax}\left(\frac{\tilde{\mathbf{Z}} \tilde{\mathbf{M}}_A^T}{\tau}\right) \in \mathbb{R}^{(B_a T) \times K}. \quad (10)$$

$$\mathbf{u} = \frac{1}{B_a T} \mathbf{1}^T \mathbf{Q} \in \mathbb{R}^K. \quad (11)$$

(i) *Domain alignment* We align real Normal and pseudo-Normal distributions through adversarial training. Let  $\bar{\mathbf{f}}_N$  and  $\bar{\mathbf{f}}_{\tilde{N}}$  denote the mean features of Normal and pseudo-Normal streams, and  $D(\cdot)$  the domain discriminator with gradient reversal layer  $G_{\lambda_{\text{da}}}(\cdot)$ . The domain alignment loss is

$$\begin{aligned} \mathcal{L}_{\text{DA}} = & \text{BCE}(D(G_{\lambda_{\text{da}}}(\bar{\mathbf{f}}_N)), y_N) \\ & + \text{BCE}(D(G_{\lambda_{\text{da}}}(\bar{\mathbf{f}}_{\tilde{N}})), y_{\tilde{N}}) \\ & + \lambda_{\text{dist}} \|\bar{\mathbf{f}}_N - \bar{\mathbf{f}}_{\tilde{N}}\|_2^2, \end{aligned} \quad (12)$$

where  $\lambda_{\text{da}} \geq 0$  controls the gradient reversal strength and  $\lambda_{\text{dist}} \geq 0$  weights the explicit Normal–pseudo-Normal feature alignment term.

(ii) *Usage-aware update.* While domain alignment adjusts global statistics, some slots may remain underutilized. Let  $\mu_k = (\sum_n Q_{nk} \mathbf{Z}_n) / (\sum_n Q_{nk})$  be the responsibility-weighted center of slot  $k$ ,  $\mathbf{m}_k$  the  $k$ -th row of  $\mathbf{M}_A$ , and  $\bar{u} = \frac{1}{K} \sum_k u_k$  the mean slot usage. We encourage balanced coverage by pulling underused slots more strongly toward their centers:

$$\mathcal{L}_{\text{upd}} = \frac{1}{K} \sum_{k=1}^K \left( \frac{\bar{u}}{u_k + \varepsilon} \right)^\beta \|\mathbf{m}_k - \mu_k\|_2^2. \quad (13)$$

**Objective.** Our final loss augments the UR-DMU discrimination term with the three regularizers:

$$\mathcal{L} = \mathcal{L}_{\text{UR-DMU}} + \lambda_1 \mathcal{L}_{\text{DA}} + \lambda_2 \mathcal{L}_{\text{upd}} \quad (14)$$

## 4. Experiments

### 4.1. Experimental Setup

**Setup.** Unless otherwise specified, we follow an *unsupervised training* regime: the training data include only real normal videos and the names of abnormal classes that might appear at inference time; *no real abnormal videos* are used for training. At evaluation, both real normal and real abnormal videos are included, and we report frame-level metrics.

**Datasets.** We evaluate on two widely used benchmarks with distinct characteristics: ShanghaiTech (SHT) [9] and UCF-Crime (Crime) [16]. SHT consists of fixed-view campus surveillance scenes with diverse illumination and viewpoints, spanning 13 locations and 437 video clips, and covering 14 abnormal categories (e.g., bicycle riding, skateboard intrusion, fighting), with 63 abnormal clips available in the training split. Following common practice for weakly supervised evaluation[5, 11, 19], we use the revised

Table 2. Examples of prompt refinement by the VLM. The refined prompt adds scene-consistent details while keeping the abnormal concept explicit.

w/o refine	Generate Shoplifting
w/ refine	Generate Store theft involves an individual removing merchandise from shelves, concealing it in a backpack, and evading surveillance cameras.



Figure 6. Initial image examples produced by our CLIP-based selection for SHT and UCF-Crime. Images are class-relevant and scene-consistent, serving as anchors for I2V synthesis.

split of [29] at test time, while keeping training *abnormal-free*. For SHT, we synthesize 10 pseudo-abnormal clips per class (total 140) and additionally generate 50 pseudo-normal clips for domain alignment.

Crime is a large-scale collection of real-world surveillance videos (about 1,900 videos,  $\sim 128$  hours) covering 13 abnormal classes (e.g., explosion, abuse), with 800 abnormal clips in the training split. For Crime, we synthesize 20 pseudo clips per class (total 260) and additionally generate 80 pseudo-normal clips. Following prior setups[32], we apply 10-crop augmentation; details of pseudo-generation are provided in the supplementary material.

**Metrics.** To assess the *generation quality* of the synthesized videos, we report standard video generation metrics. For image-level quality, we compute Fréchet Inception Distance (FID) and Kernel Inception Distance (KID) between frame distributions of generated and real videos. For spatiotemporal fidelity, we report Fréchet Video Distance (FVD) and Kernel Video Distance (KVD) based on I3D features, capturing motion and temporal coherence. For *anomaly detection*, we follow the VAD literature and report frame-level Area Under the ROC Curve (AUC).

**Implementation Details.** We use the Wan 2.2 image-to-video diffusion model (I2V-A14B) [20] with a resolution of  $832 \times 480$  and a frame length of 81. For prompt refinement, we employ the Qwen3 30B-A3B vision-language model [23]. As an auxiliary video feature extractor (for analysis/metrics), we use the final projector embedding (3,584-D) of Qwen2.5-VL 7B-Instruct [1]. CLIP ViT-B/32 [13] is used for initial image selection. Our implementation is based on PyTorch and HuggingFace Transformers. **Initial Images and Prompt Design.** Using the init selection process in Sec. 3.1.1, we obtain class-relevant init images for SHT and Crime (Fig. 6). They exhibit minimal

semantic mismatch to target classes. Representative examples of VLM-based prompt refinement are shown in Table 2, where the refined text better reflects the scene context of the initial image. These inits and refined prompts are then fed to the I2V generator to construct the pseudo-anomaly datasets. Please refer to the supplementary material for the detail.

## 4.2. Qualitative Evaluation

### Class-Aware Pseudo-Anomaly Generator (CA-PAG)

Fig. 7 shows examples of generated videos. Without prompt refinement (*w/o Refine*, i.e., using the raw class label), ambiguous instructions degrade consistency and text-video alignment, leading in SHT to artifacts such as the intrusion of large fighting crowds, object merging/disappearance across frames, and excessive motion that ignores physical plausibility. On Crime, we likewise observe multiple vehicles appearing/disappearing. With prompt refinement (*w/ Refine*), the VLM-guided prompts produce scenes that reflect the initial image context: on SHT we observe person-person fighting present in the initial image with more natural motion; on Crime we observe an inter-vehicle collision without disappearance/merging artifacts.

**Domain-Aligned Regularized Module(DARM).** Fig. 8 shows score traces (vertical: score; horizontal: time). Left: in “skateboard intrusion,” *w/ DARM* responds sharply at abnormal segments, while *w/o DARM* barely rises. In the “biker” case, *w/ DARM* suppresses false positives and concentrates its peak within the annotated interval. Right: in “explosion,” *w/ DARM* sustains higher sensitivity during the burning phase. In “burglary,” it produces temporally tighter peaks aligned with abnormal actions. These examples demonstrate that DARM not only enhances responsiveness to true abnormal events but also suppresses magnitude-driven false negatives, yielding temporally sharper and more semantically aligned detection peaks.

## 4.3. Quantitative Evaluation

**Pseudo-anomaly videos quality.** Table 3 reports SHT generation quality. As prompt refinement is applied, all metrics improve. In particular, we observe a reduction of FVD by -96 points and KVD by -22.4 points, indicating better motion and temporal coherence. These gains are consistent with the qualitative trends in Fig. 6, suggesting that refined prompts enhance physical plausibility and scene consistency. In contrast, KID remains unchanged. As it reflects per-frame appearance rather than temporal dynamics, both settings share nearly identical image statistics, while CA-PAG mainly improves motion coherence captured by FVD/KVD.

Table 3. Quality of pseudo-anomaly videos.

Data	FVD↓	FID↓	KVD↓	KID↓
Ours w/o Refine	701	83.9	57.4	<b>0.03</b>
Ours w/ Refine	<b>604</b>	<b>78.0</b>	<b>34.7</b>	<b>0.03</b>



Figure 7. Qualitative examples of synthesized pseudo anomalies. Top: SHT (fighting). Bottom: UCF-Crime (road accidents).

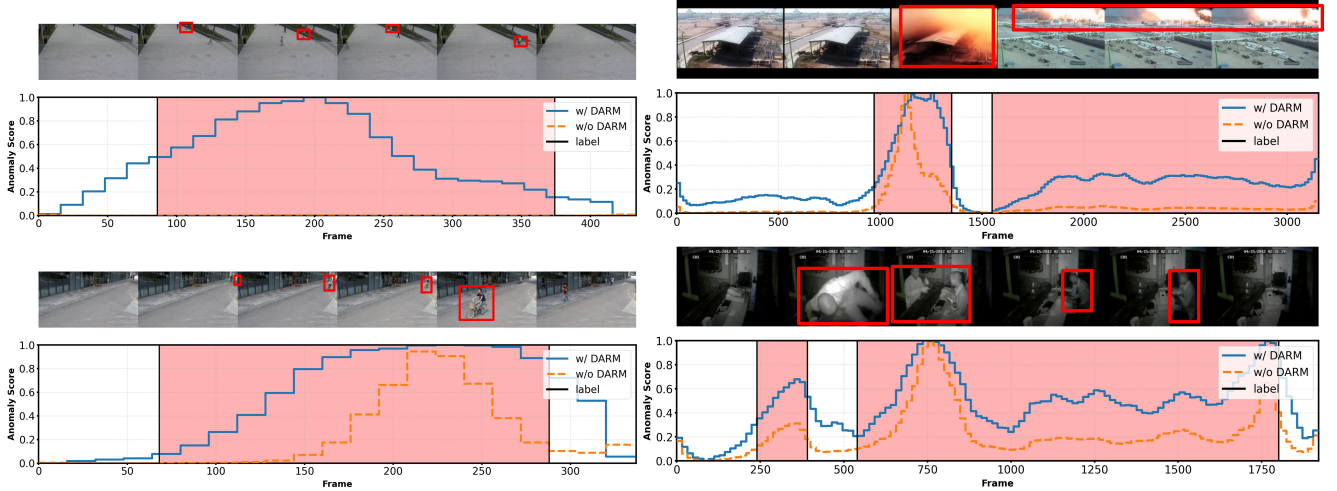


Figure 8. Qualitative detection results. Left: SHT (top:skateboarder, bottom:biker). Right: UCF-Crime (top:explosion,bottom:burglary). The adaptive memory module mitigates MIL bias and improves sensitivity to subtle abnormal segments.

**DARM for detection.** Table 4 summarizes frame-level AUC compared to prior UVAD and WVAD methods. On SHT, our PA-VAD framework with DARM achieves 98.2% AUC, outperforming the best UVAD method [6] and even surpassing the strongest WVAD competitor [5] (97.6%) by **+0.6** points, despite using *no* real abnormal videos for training. On UCF-Crime, our Real/Pseudo setting is naturally disadvantaged against Real/Real baselines, yet PA-VAD with DARM remains competitive. Importantly, UVAD methods operate under the same constraint as ours—without any real abnormal footage—making this comparison fully fair. Under this setup, PA-VAD with DARM still surpasses the UVAD state-of-the-art [30] (80.6%) by **+1.9** points. Within our PA-VAD framework, replacing the plain UR-DMU\* classifier with DARM consistently improves performance un-

der the same Real/Pseudo setting, from 96.0%  $\rightarrow$  98.2% on SHT and 80.2%  $\rightarrow$  82.5% on UCF-Crime, indicating that domain alignment and usage-aware memory shaping are crucial to fully exploiting pseudo anomalies without overfitting to their magnitude bias. Table 5 disentangles the contributions of CA-PAG and DARM on SHT. Enabling prompt refinement on top of init image selection already improves AUC from 94.9% to 96.0%, indicating that class-aware textual conditioning is important even without any regularization on the detector side. Within DARM, the usage-aware memory update is the primary driver of gains: adding the update term on top of CA-PAG boosts AUC to 97.6–97.7%, whereas domain alignment alone provides only modest improvement. The best result (98.2%) is obtained when domain alignment and usage-aware update are combined, supporting our design that DARM sup-



Table 4. Frame-level AUC (%) comparison on ShanghaiTech (SHT) and UCF-Crime. The “Data type (Nor/Abn)” column specifies whether a method uses real normal, real abnormal, or pseudo-abnormal videos.

Protocol	Methods	Reference	Data type (Nor/Abn)	SHT(%)	UCF-Crime(%)
UVAD	HF <sup>2</sup> -VAD [10]	ICCV21	Real/-	76.2	–
	LERF [17]	AAAI23	Real/-	78.6	–
	HSC [18]	CVPR23	Real/-	83.4	78.3
	MGSTRL [30]	CVPR24	Real/-	85.1	80.6
	SeeKer [6]	ICCV25	Real/-	85.5	–
WVAD	Sultani et al. [16]	CVPR18	Real/Real	85.3	75.4
	RTFM [19]	ICCV21	Real/Real	97.2	84.3
	CMRL [5]	CVPR23	Real/Real	97.6	86.1
	UMIL [11]	CVPR23	Real/Real	96.8	86.8
	UR-DMU [32]	AAAI23	Real/Real	–	87.0
	VERA [24]	CVPR25	Real/Real	–	86.6
	Ours w/UR-DMU* [32]		Real/Pseudo	96.0	80.2
PA-VAD	Ours w/DARM		Real/Pseudo	<b>98.2</b>	<b>82.5</b>

presses the pseudo-induced magnitude bias by simultaneously reducing the real/pseudo discrepancy and preventing a few high-magnitude prototypes from monopolizing MIL optimization. Table 6 further analyzes robustness to the amount of synthesized data on SHT. Increasing the number of pseudo-abnormal clips from 14 to 140 steadily improves performance from 85.4% to 98.2% AUC, and we already reach 96.9% with only 70 clips. Even when the number of synthesized clips is reduced to around the scale of the 63 real abnormal clips in the standard WVAD split, PA-VAD with DARM remains highly competitive. When we further increase the number of synthesized clips to 175, the AUC slightly drops to 97.7%, suggesting a mild saturation effect where overly many pseudo clips introduce redundancy or noise that does not further benefit, and can slightly harm, generalization. Overall, the results indicate that pseudo-only training can match or exceed Real/Real pipelines, offering a practical option when abnormal data is unavailable.

**Limitation.** On UCF-Crime, our method does not surpass the SoTA that trains with real abnormal videos under the WVAD setup. A likely factor is the difficulty of synthesizing minute-long, context-heavy anomalies (e.g., extended temporal dependencies), which remain challenging for current video generators; such anomalies are more prevalent in UCF-Crime than in SHT, making the dataset inherently harder under a pseudo-only setting.

## 5. Conclusion

We presented PA-VAD, a pseudo-only anomaly detection framework built on two components: the Class-Aware Pseudo-Anomaly Generator (CA-PAG) for synthesizing

Table 5. Ablation table for CA-PAG and DARM components.

CA-PAG		DARM		AUC(%)
Initial	Refine	DA	Update	
✓				94.9
✓	✓			96.0
✓			✓	97.6
✓	✓		✓	97.7
✓		✓		96.0
✓	✓	✓		96.8
✓	✓	✓	✓	<b>98.2</b>

Table 6. Effect of the number of synthesized clips on SHT. We vary the number of generated pseudo-abnormal clips (total = 140) and report the frame-level AUC (%).

Clips	14	35	70	105	140	175
SHT (%)	85.4	94.6	96.9	97.3	<b>98.2</b>	97.7

class-consistent pseudo anomalies and the Domain-Aligned Regularized Module (DARM) for mitigating magnitude bias and stabilizing learning. Despite using no real abnormal footage, PA-VAD achieves competitive or superior performance to strong baselines on SHT and UCF-Crime, showing that high-quality pseudo anomalies combined with domain alignment can serve as a practical alternative to Real/Real pipelines. Future work includes extending CA-PAG to richer motion priors and evaluating PA-VAD with broader video generative models.

## References

- [1] Shuai Bai et al. Qwen2.5-vl technical report. *arXiv preprint arXiv:2502.13923*, 2025. 6
- [2] Andreas Blattmann, Tim Dockhorn, Sumith Kulal, Daniel Mendelevitch, Maciej Kilian, Dominik Lorenz, Yam Levi, Zion English, Vikram Voleti, Adam Letts, Varun Jampani, and Robin Rombach. Stable Video Diffusion: Scaling Latent Video Diffusion Models to Large Datasets. *arXiv preprint arXiv:2311.15127*, 2023. 3
- [3] Shijie Cai, Xiaolin Peng, Chenyang Wang, Xinyu Cai, and Jian Qian. Gv-vad: Exploring video generation for weakly-supervised video anomaly detection. *arXiv preprint arXiv:2508.00312*, 2025. 2, 3
- [4] Haoxin Chen, Yong Zhang, Xiaodong Cun, Menghan Xia, Xintao Wang, Chao Weng, and Ying Shan. VideoCrafter2: Overcoming Data Limitations for High-Quality Video Diffusion Models. In *Proc. of CVPR*, 2024. 3
- [5] MyeongAh Cho, Minjung Kim, Sangwon Hwang, Chaewon Park, Kyungjae Lee, and Sangyoun Lee. Look Around for Anomalies: Weakly-Supervised Anomaly Detection via Context-Motion Relational Learning. In *Proc. of CVPR*, 2023. 1, 2, 5, 7, 8
- [6] Anja Delić, Matej Grčić, and Siniša Šegvić. Sequential key-point density estimator: an overlooked baseline of skeleton-based video anomaly detection. In *Proc. of ICCV*, 2025. 1, 7, 8
- [7] Hang Du, Sicheng Zhang, Binzhu Xie, Guoshun Nan, Jiayang Zhang, Junrui Xu, Hangyu Liu, Sicong Leng, Jiangming Liu, Hehe Fan, Dajiu Huang, Jing Feng, Linli Chen, Can Zhang, Xuhuan Li, Hao Zhang, Jianhang Chen, Qimei Cui, and Xiaofeng Tao. Uncovering what, why and how: A comprehensive benchmark for causation understanding of video anomaly. In *Proc. of CVPR*, 2024. 1, 3
- [8] Yushi Hu, Zeyu Liu, Hang Zhang, Trevor Darrell, Alexei A. Efros, et al. TIFA: Accurate and Interpretable Text-to-Image Faithfulness Evaluation with Question Answering. In *Proc. of ICCV*, 2023. 4
- [9] Wen Liu, Weixin Luo, Dongze Lian, and Shenghua Gao. Future Frame Prediction for Anomaly Detection – A New Baseline. In *Proc. of CVPR*, 2018. 1, 2, 5
- [10] Zhian Liu, Yongwei Nie, Chengjiang Long, Qing Zhang, and Guiqing Li. A Hybrid Video Anomaly Detection Framework via Memory-Augmented Flow Reconstruction and Flow-Guided Frame Prediction. In *Proc. of ICCV*, 2021. 1, 2, 8
- [11] Hui Lv, Zhongqi Yue, Qianru Sun, Bin Luo, Zhen Cui, and Hanwang Zhang. Unbiased Multiple Instance Learning for Weakly Supervised Video Anomaly Detection. In *Proc. of CVPR*, 2023. 1, 2, 5, 8
- [12] Ninareh Mehrabi, Chiyuan Zhang, Helen Toner, Emre Kiciman, et al. Resolving Ambiguities in Text-to-Image Generative Models. In *Proc. of ACL*, 2023. 4
- [13] Alec Radford, Jong Wook Kim, Chris Hallacy, Aditya Ramesh, Gabriel Goh, Sandhini Agarwal, Girish Sastry, Amanda Askell, Pamela Mishkin, Jack Clark, Gretchen Krueger, and Ilya Sutskever. Learning transferable visual models from natural language supervision. In *Proc. of ICML*, 2021. 4, 6
- [14] Ayush K. Rai, Tarun Krishna, Feiyan Hu, Alexandru Drimborean, Kevin McGuinness, Alan F. Smeaton, and Noel E. O’Connor. Video anomaly detection via spatio-temporal pseudo-anomaly generation: A unified approach. In *Proc. of CVPRw*, 2024. 2, 3
- [15] Huamin Ren, Weifeng Liu, Søren Ingvor Olsen, Sergio Escalera, and Thomas B Moeslund. Unsupervised Behavior-Specific Dictionary Learning for Abnormal Event Detection. In *Proc. of BMVC*, 2015. 1, 2
- [16] Waqas Sultani, Chen Chen, and Mubarak Shah. Real-world Anomaly Detection in Surveillance Videos. In *Proc. of CVPR*, 2018. 1, 2, 4, 5, 8
- [17] Che Sun, Chenrui Shi, Yunde Jia, and Yuwei Wu. Learning Event-Relevant Factors for Video Anomaly Detection. In *Proc. of AAAI*, 2023. 1, 2, 8
- [18] Shengyang Sun and Xiaojin Gong. Hierarchical Semantic Contrast for Scene-Aware Video Anomaly Detection. In *Proc. of CVPR*, 2023. 1, 2, 8
- [19] Yu Tian, Guansong Pang, Yuanhong Chen, Rajvinder Singh, Johan W Verjans, and Gustavo Carneiro. Weakly-Supervised Video Anomaly Detection With Robust Temporal Feature Magnitude Learning. In *Proc. of ICCV*, 2021. 1, 2, 5, 8
- [20] Team Wan and et al. Wan: Open and advanced large-scale video generative models. *arXiv preprint arXiv:2503.20314*, 2025. 3, 6
- [21] Peng Wu, Xuerong Zhou, Guansong Pang, Lingru Zhou, Qingsen Yan, Peng Wang, and Yanning Zhang. Open-Vocabulary Video Anomaly Detection. In *Proc. of CVPR*, 2024. 1, 2
- [22] Peng Wu, Xuerong Zhou, Guansong Pang, Lingru Zhou, Qingsen Yan, Peng Wang, and Yanning Zhang. VadCLIP: Adapting Vision-Language Models for Weakly Supervised Video Anomaly Detection. In *Proc. of AAAI*, 2024. 1, 2
- [23] An Yang et al. Qwen3 technical report. *arXiv:2505.09388*, 2025. 6
- [24] Muchao Ye, Weiyang Liu, and Pan He. Vera: Explainable video anomaly detection via verbalized learning of vision-language models. In *Proc. of CVPR*, 2025. 1, 8
- [25] Guang Yu, Siqi Wang, Zhiping Cai, Xinwang Liu, Chuanfu Xu, and Chengkun Wu. Deep Anomaly Discovery From Unlabeled Videos via Normality Advantage and Self-Paced Refinement. In *Proc. of CVPR*, 2022. 1, 2
- [26] M Zaigham Zaheer, Arif Mahmood, M Haris Khan, Mattia Segu, Fisher Yu, and Seung-Ik Lee. Generative Cooperative Learning for Unsupervised Video Anomaly Detection. In *Proc. of CVPR*, 2022. 1, 2
- [27] Chen Zhang, Guorong Li, Yuankai Qi, Shuhui Wang, Laiyun Qing, Qingming Huang, and Ming-Hsuan Yang. Exploiting Completeness and Uncertainty of Pseudo Labels for Weakly Supervised Video Anomaly Detection. In *Proc. of CVPR*, 2023. 1, 2
- [28] Huaxin Zhang, Xiaohao Xu, Xiang Wang, Jialong Zuo, Xiaonan Huang, Changxin Gao, Shanjun Zhang, Li Yu, and Nong Sang. Holmes-vau: Towards long-term video anomaly understanding at any granularity. In *Proc. of CVPR*, 2025. 1, 3

- [29] Jiangong Zhang, Laiyun Qing, and Jun Miao. Temporal Convolutional Network with Complementary Inner Bag Loss for Weakly Supervised Anomaly Detection. In *Proc. of ICIP*, 2019. [6](#)
- [30] Menghao Zhang, Jingyu Wang, Qi Qi, Haifeng Sun, Zirui Zhuang, Pengfei Ren, Ruilong Ma, and Jianxin Liao. Multi-Scale Video Anomaly Detection by Multi-Grained Spatio-Temporal Representation Learning. In *Proc. of CVPR*, 2024. [1](#), [2](#), [7](#), [8](#)
- [31] Jia-Xing Zhong, Nannan Li, Weijie Kong, Shan Liu, Thomas H Li, and Ge Li. Graph Convolutional Label Noise Cleaner: Train a Plug-And-Play Action Classifier for Anomaly Detection. In *Proc. of CVPR*, 2019. [1](#), [2](#)
- [32] Hang Zhou, Junqing Yu, and Wei Yang. Dual memory units with uncertainty regulation for weakly supervised video anomaly detection. In *Proc. of AAAI*, 2023. [1](#), [2](#), [5](#), [6](#), [8](#)



# Pseudo Anomalies Are All You Need: Diffusion-Based Generation for Weakly-Supervised Video Anomaly Detection

## Supplementary Material

### S1. Additional Details of CA-PAG

#### S1.1 Initial image retrieval

For each abnormal class  $c$ , we retrieve an initial image from the training set of real normal videos that is visually compatible with the target abnormal context. Concretely, we first construct a positive query sentence  $q_c^+$  that describes a class-relevant surveillance scene, and a negative query  $q_c^-$  that filters out non-surveillance artefacts such as noisy images or logos. Example phrases of "road accidents" include:

- Positive: "road accidents, roadway, multiple vehicles, street lanes, intersection, traffic lights, road shoulder, median strip, daytime or dusk, fixed high pole camera, moderate motion blur"
- Negative: "dashboard ui overlay, speedometer close-up, racing circuit"

We encode all candidate normal frames and both queries using CLIP, and compute similarity between each frame and  $q_c^+$  while penalizing similarity to  $q_c^-$ . Figure 9 in the supplementary material visualizes examples of retrieved init images for "road accidents" class of UCF-Crime[16]. This CLIP-based retrieval anchors the synthesis process to class-consistent, surveillance-style scenes without requiring any real abnormal footage.



Figure 9. Top-4 retrieved init images for the class "road accident". Ranking is left to right (1st→4th).

#### S1.2 Prompt refinement with a VLM

Starting from a coarse abnormal class name (e.g., "fighting", "robbery"), we construct an initial English prompt that describes the abnormal event in a surveillance setting.

Given an init image  $x$  and a coarse textual description  $p_c^{\text{coarse}}$ , we query the VLM with an instruction that (i) asks for a more detailed, temporally grounded description of the abnormal event, (ii) explicitly constrains the camera to be static, and (iii) enforces scene consistency with the given surveillance image. A simple example is as follows:

You are an expert in visual scene understanding and anomaly-behavior design. Given an input image and an anomaly category, describe the most plausible abnormal behavior consistent with both the scene and the category. Your output

must be a single short sentence completing the pattern "Generate abuse behavior, manifested as ...". Use only elements clearly visible in the image. Do not invent unseen objects, persons, weapons, or motions. Keep the action realistic, scene-grounded, and visually justified. Camera motion is strictly prohibited.

We provide the full VLM instruction prompt (written in Chinese) used for textual refinement in the supplementary material. The VLM outputs a refined prompt  $p_c^{\text{refined}}(x)$  that is used to condition the video diffusion model. Table 7 shows examples of coarse vs. refined prompts. Typically, the refined prompt adds temporal structure (e.g., gradual approach, interaction, and departure), clarifies the role of normal bystanders, and explicitly states the absence of camera motion, which stabilizes the synthesized videos.

Table 7. Examples of prompt refinement used in CA-PAG.

Before Refinement	After Refinement
Generate <b>abuse</b> .	Generate a person in an office space aggressively shoves and restrains another individual at close distance.
Generate <b>burglary</b> .	Generate a person reaches behind a store counter to rummage through items while another stands watching from the front.
Generate <b>robbery</b> .	Generate in a parking lot, an individual approaches near a vehicle and forcibly grabs an item from another person.

#### S1.3 Pseudo-anomaly generation with Wan2.2

We use an image-to-video diffusion model (Wan2.2) to synthesize pseudo-abnormal clips conditioned on the init image and the refined prompt. Unless otherwise stated, we use a resolution of  $832 \times 480$  pixels, 81 frames per clip, a frame rate of 16 fps, and 25 sampling steps. These settings are shared across classes for both ShanghaiTech and UCF-Crime. For the classifier-free guidance scale, we use (3.5, 3.5) for SHT and (6.5, 4.5) for UCF-Crime.

Figure 10 illustrates representative synthesized clips for four classes (burglary, explosion, moving car, vandalism) and one failure case (shoplifting). We observe that short, visually localized anomalies (e.g., explosions around a single object, brief collisions, or localized vehicle motion) are synthesized with high fidelity and maintain a consistent surveillance viewpoint. In contrast, long-horizon, context-heavy

<sup>0</sup>Original prompts were written in Chinese before translation and refinement.



(a) Burglary (UCF-Crime)



(b) Explosion (UCF-Crime)



(c) Moving car (ShanghaiTech)



(d) Vandalism (UCF-Crime)



(e) Shoplifting (UCF-Crime, failure example)

Figure 10. Representative synthesized pseudo-anomaly examples used in PA-VAD. Four high-fidelity cases (burglary, explosion, moving car, vandalism) and one failure case (shoplifting), where the abnormal cue remains vague or partially missing.

crimes such as shoplifting or subtle abuse are more difficult: the generator often produces largely normal behavior with only vague or missing abnormal cues. We explicitly treat such failure cases as part of the pseudo-anomaly distribution; DARM is designed to tolerate these imperfections and to prevent a few high-magnitude but unfaithful clips from dominating MIL optimization.

## S2. Additional Details of DARM

### 5.1. Loss Terms and Coefficients

Our final training loss follows Eq. (14) of the main paper:

$$\mathcal{L} = \mathcal{L}_{\text{UR-DMU}} + \lambda_1 \mathcal{L}_{\text{DA}} + \lambda_2 \mathcal{L}_{\text{upd}},$$

where each coefficient corresponds to:

- $\lambda_1$ : weight for the domain-alignment loss  $\mathcal{L}_{\text{DA}}$  (Eq. (12))
- $\lambda_2$ : weight for the usage-aware memory update loss  $\mathcal{L}_{\text{upd}}$  (Eq. (13))
- $\lambda_{\text{da}}$ : gradient reversal strength in Eq. (12)
- $\lambda_{\text{dist}}$ : explicit Normal–pseudo-Normal alignment term in Eq. (12)
- $\beta$ : exponent controlling the scaling of usage-aware correction in Eq. (13)

All hyperparameters used in the main experiments are summarized in Table 8.

## S3. Computational Cost

### S3.1 Generation cost

All pseudo-anomaly and pseudo-normal videos in our experiments are generated with Wan2.2 on a workstation running Ubuntu 24.04.3 LTS equipped with a single NVIDIA RTX 6000 Ada 100 GB GPU. During synthesis, Wan2.2 utilizes approximately 95,776 MiB of GPU memory, and generating a single pseudo-anormal clip takes about 9 minutes 35 seconds. Producing all synthesized clips for ShanghaiTech (140 pseudo-anormal and 50 pseudo-normal clips) requires roughly 30 hours of wall-clock time, while the full set for UCF-Crime (260 pseudo-anormal and 80 pseudo-normal clips) takes about 55 hours. Considering the scarcity and privacy constraints of real abnormal footage, this generation cost remains modest; PA-VAD enables efficient large-scale pseudo-anomaly creation, offering a practical and scalable alternative to collecting real anomalies.

Table 8. Training hyperparameters for SHT and UCF-Crime. All experiments use the same backbone, data pipeline, and MIL configuration; only dataset-dependent constants differ.

Hyperparameter	ShanghaiTech	UCF-Crime
Batch size	4	4
Learning rate	$1 \times 10^{-4}$	$1 \times 10^{-5}$
Segment number	5	64
Optimizer	Adam	Adam
weight decay	$1 \times 10^{-5}$	$1 \times 10^{-5}$
$\lambda_1$ (Eq. 14, weight of $\mathcal{L}_{DA}$ )	1.0	1.0
$\lambda_2$ (Eq. 13, weight of $\mathcal{L}_{upd}$ )	0.1	0.1
$\lambda_{da}$ (Eq. 12, GRL strength)	0.2	0.1
$\lambda_{dist}$ (Eq. 12, N- $\tilde{N}$ distance)	0.01	0.01
$\beta$ (Eq. 13, usage exponent)	1.0	1.0
Abnormal memory slots $K_{abn}$	100	60
Normal memory slots $K_{norm}$	100	60